Reliable conjunctive use rules for sustainable irrigated agriculture and reservoir spill control

Gerrit Schoups,[1] C. Lee Addams,[1,2] Jose Luis Minjares,[3] and Steven M. Gorelick[1]

Received 1 March 2006; revised 2 August 2006; accepted 21 August 2006; published 14 December 2006.

[1] We develop optimal conjunctive use water management strategies that balance two potentially conflicting objectives: sustaining irrigated agriculture during droughts and minimizing unnecessary spills and resulting water losses from the reservoir during wet periods. Conjunctive use is specified by a linear operating rule, which determines the maximum surface water release as a function of initial reservoir storage. Optimal strategies are identified using multiobjective interannual optimization for sustainability and spill control, combined with gradient-based annual profit maximization. Application to historical conditions in the irrigated system of the Yaqui Valley, Mexico, yields a Pareto curve of solutions illustrating the trade-off between sustaining agriculture and minimizing spills and water losses. Minimal water losses are obtained by maximizing surface water use and limiting groundwater pumping, such that reservoir levels are kept sufficiently low. Maximum agricultural sustainability, on the other hand, results from increased groundwater use and keeping surface water reservoir levels high during wet periods. Selected optimal operating rules from the multiobjective optimization are tested over a large number of equally probable streamflow time series, generated with a stochastic time series model. In this manner, statistical properties, such as the mean sustainability and sustainability percentiles, are determined for each optimal rule. These statistical properties can be used to select rules for water management that are reliable over a wide range of streamflow conditions.

Citation: Schoups, G., C. L. Addams, J. L. Minjares, and S. M. Gorelick (2006), Reliable conjunctive use rules for sustainable irrigated agriculture and reservoir spill control, *Water Resour. Res.*, *42*, W12406, doi:10.1029/2006WR005007.

1. Introduction

[2] Conjunctive use of surface water and groundwater resources for irrigated agriculture is beneficial because it can buffer the natural variability of supplies obtained from surface water by relying to a greater extent on groundwater, which is typically more expensive. In many arid and semiarid regions, surface water reservoirs have been built to protect against the natural variability of runoff. However, reservoirs constructed for drought mitigation usually perform multiple tasks that conflict with water supply for irrigation, such as flood protection [*Yeh*, 1985; *Labadie*, 2004]. Groundwater provides additional insurance against reductions in agricultural production during droughts [*Bredehoeft and Young*, 1983; *Tsur*, 1990]. A drawback is that increased groundwater pumping during extended droughts may lead to severe aquifer head drawdowns, resulting in high pumping costs and seawater intrusion in coastal aquifers [*Willis and Finney*, 1988; *Reichard and Johnson*, 2005; *Schoups et al.*, 2006]. When developing conjunctive water management strategies, all these issues should be taken into account. In addition, given the large uncertainty in surface water supply, the proposed strategies should be reliable over a wide range of streamflow scenarios. Therefore a two-pronged approach is needed. First, a tool is needed to quantify streamflow uncertainty, which is commonly achieved by means of a stochastic streamflow model. Second, optimal water management decisions need to be identified that account for streamflow uncertainty, which results in a stochastic optimization problem.

[3] The literature on stochastic time series analysis applied to streamflow modeling is vast and many methods have been developed for a wide range of problems [*Salas*, 1993]. In this paper, we are concerned with the concurrent generation of monthly streamflow at multiple reservoirs such that observed autocorrelations and cross correlations are preserved at both monthly and multiannual timescales. Particularly, in terms of sustainable water management it is essential that the observed drought characteristics are preserved in the generated time series [*Loaiciga*, 2005]. Either parametric or nonparametric methods may be used for this type of problem. Parametric models make assumptions about the form of the distributions (e.g., Gaussian) and typically require a large number of parameters to be estimated when both short-term and long-term correlations need to be preserved [*Rasmussen et al.*, 1996]. Parametric disaggregation methods [*Koutsoyiannis*, 2001] are available to deal with this problem by e.g., first generating annual streamflows, followed by disaggregation to monthly flows.

[1]Department of Geological and Environmental Sciences, Stanford University, Stanford, California, USA.
[2]International Research Institute for Climate Prediction, Earth Institute, Columbia University, Palisades, New York, USA.
[3]Comisión Nacional del Agua, Cuidad Obregón, Mexico.

0043-1397/06/2006WR005007$09.00

Alternatively, nonparametric models such as bootstrapping methods [*Vogel and Shallcross*, 1996] and kernel-based methods [*Tarboton et al.*, 1998] have been developed that do not make any prior assumptions about the shapes of the distributions. More recently, hybrid methods have been introduced that combine the strength of both parametric and nonparametric approaches [*Srinivas and Srinivasan*, 2005].

[4] The next step is to solve the problem of optimal water management under uncertain water supply. Two main approaches can be distinguished, namely implicit and explicit stochastic optimization [*Labadie*, 2004]. Implicit stochastic optimization (ISO) relies on deterministic optimization methods to find management strategies that are optimal over a long historical record [*Lund and Ferreira*, 1996] or over a large number of shorter synthetic streamflow realizations [*Young*, 1967; *Bhaskar and Whitlatch*, 1980]. Postoptimization regression analysis [*Hiew et al.*, 1989] or neural network analysis [*Raman and Chandramouli*, 1996] of the optimization results then yields general operating rules that, for example, specify reservoir releases as a function of current storage. Explicit stochastic optimization (ESO) on the other hand works directly with streamflow probabilities, which can either be included in the objective function, as in stochastic linear programming [*Jacobs et al.*, 1995; *Seifi and Hipel*, 2001] and stochastic dynamic programming [*Loaiciga and Marino*, 1986; *Tejada-Guibert et al.*, 1995; *Faber and Stedinger*, 2001], or in the constraints through chance-constrained programming [e.g., *Loucks and Dorfman*, 1975], or in both the objective function and the constraints [*Reichard*, 1995]. The ESO approach explicitly accounts for the lack of perfect knowledge of future events, but it can lead to computationally intractable optimization problems of multireservoir systems.

[5] The current paper focuses on conjunctive use in one of the most important agricultural regions in Mexico, the 6800 km^2 Yaqui Valley near the Sea of Cortez in the state of Sonora. The objective here is to derive conjunctive surface water and groundwater operating rules for a wide range of streamflow scenarios. In particular, the goal is to find a balance between unnecessary reservoir spills during wet periods and sustained irrigated agriculture during drought conditions, while avoiding excessive aquifer head drawdowns and seawater intrusion.

[6] We build on a deterministic spatially distributed numerical simulation-optimization model for the Yaqui Valley developed by *Schoups et al.* [2006], and present here for the first time an approach that involves a combination of methods enabling us to consider a more complex, multiannual, regional water management problem under uncertainty. Methodologically, *Schoups et al.* [2006] studied elements of water management with a deterministic model of the hydrologic systems (surface water reservoirs and alluvial coastal aquifer), and a model that simulates crop production. Using these model components, a series of annual profit maximization problems were solved with large-scale constrained gradient-based optimization. Unlike that prior work, here we consider a substantially different problem. We study multiobjective trade-offs in surface water reservoir operation that arise from uncertainty in streamflow. In addition, our water management model is multiannual and integrates a variety of modern methodological advances.

[7] There are three primary contributions of the current work. First, water management operating rules are identified in a hierarchical framework by means of interannual optimization of agricultural sustainability and spill minimization using a multiobjective global optimization algorithm [*Vrugt et al.*, 2003], with a nested series of annual profit-maximizing models solved with nonlinear gradient-based optimization [*Gill et al.*, 2002]. As a starting point, our hierarchical optimization framework was based on the approach of *Cai et al.* [2001], who used a genetic algorithm for multiannual optimization and linear programming for annual optimization. Ours is a nonlinear optimization problem and therefore the approach is a generalization of the one presented by Cai et al. However, more importantly, our problem is a multiobjective one. Cai et al. considered only one objective, namely agricultural sustainability. Our approach on the other hand, explicitly quantifies trade-offs between two objectives: sustaining irrigated agriculture during droughts and minimizing unnecessary reservoir losses during wet periods. Our study also builds upon the valuable approach of *Lund and Ferreira* [1996]. As in their work, we assume perfect knowledge of a long historical record of monthly streamflows. However, our approach differs from that study in that optimal management is parameterized by a linear operating rule. Our method is similar to the piecewise linear operating rules of *Oliveira and Loucks* [1997]. The slope and intercept of the linear rule are used as decision variables in the multiannual optimization. A second contribution of this paper that was not within the scope of *Schoups et al.* [2006] is that uncertainty in surface water supply is quantitatively addressed. To accomplish this, we use a large number of equally probable streamflow realizations generated by the stochastic streamflow generation method of *Srinivas and Srinivasan* [2005]. Our third contribution involves performance evaluation. Optimal operating rules are evaluated by means of a postoptimization Monte Carlo analysis using a large set of generated streamflow records. In that sense, our approach is related to the implicit stochastic optimization (ISO) method discussed earlier.

[8] The paper is organized as follows. First, we give some background on the Yaqui Valley study area. This is followed by an outline of the hierarchical optimization approach, and a brief discussion of the stochastic streamflow model. Results are then presented for each part of the analysis and finally our findings are summarized in the conclusions.

2. Yaqui Valley Study Area

[9] The Yaqui Valley is located in the southern part of the state of Sonora, Mexico. It consists of a coastal alluvial plain bordered by the Sea of Cortez and the Sierra Madre Mountains. The climate is semiarid with annual potential evapotranspiration (2000 mm) much larger than annual precipitation (300 mm). Farmers in the Yaqui Valley are organized into an irrigation district, which we will refer to as ''the district''. Wheat is the dominant crop and is grown from November to April. Irrigation mainly depends on surface water from the Yaqui River, which is stored in three sequential reservoirs with a total capacity of 6713×10^6 m^3. Surface water is distributed to farms in the district by means of a network of irrigation canals, most of which are unlined. Although available water storage in the alluvial aquifer underlying the district (estimated at $100{,}000 \times 10^6$ m^3) is

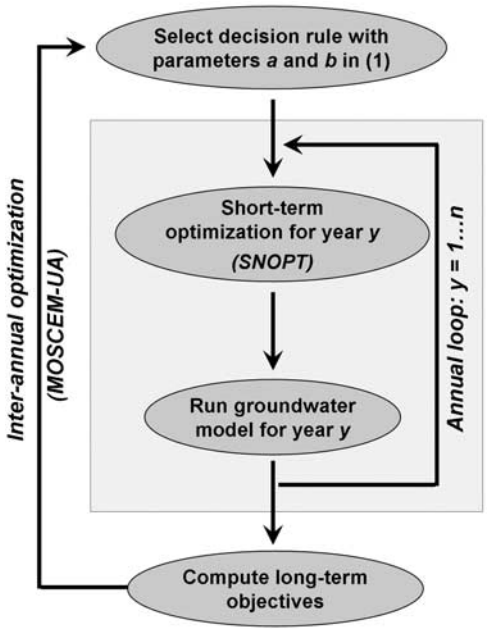

Figure 1. Schematic of the hierarchical optimization strategy: optimization occurs at the annual timescale using a nonlinear gradient-based algorithm (SNOPT), and at the interannual timescale using a global Monte Carlo–based multiobjective algorithm (MOSCEM-UA).

much larger than surface water storage, historically, groundwater pumping has been limited to approximately 400 $\times$ 10^6 m^3 per year, as supplied by almost 350 wells. Surface drainage ditches discharge excess irrigation water and fertilizer to the ocean, leading to temporary algal blooms in the Sea of Cortez [*Beman et al.*, 2005]. For further background on the hydrology of the Yaqui Valley, we refer to *Addams* [2004] and *Schoups et al.* [2005].

3. Multiscale Hierarchical Optimization Framework

[10] The optimization model operates on two timescales (Figure 1): a long-term or interannual timescale and a short-term or annual timescale. In the following sections we discuss methods, decision variables, and objectives for these two timescales.

3.1. Interannual Optimization Model

[11] The purpose of the interannual optimization model is to identify an optimal conjunctive use plan that maximizes performance indices that quantify agricultural sustainability and reservoir spills, to be defined in the next paragraph. Conjunctive use for irrigation is quantified by a linear operating or release rule of the form,

$$RA_y = a \times AS_y + b \tag{1}$$

where RA_y is annual water allocation from the downstream reservoir (Oviachic) to the district and AS_y is available storage at the end of September in year y, both in units of 10^6 m^3. Available storage is calculated as the total storage in the three reservoirs minus 1650 $\times$ 10^6 m^3, which accounts for dead storage (950 $\times$ 10^6 m^3), diversions to other users such as urban water supply, mining operations, and water obligated to prior appropriators (400 $\times$ 10^6 m^3), and evaporation (300 $\times$ 10^6 m^3). Coefficients a and b are slope and intercept, respectively, of the linear operating rule. When a is zero, b represents an upper limit on annual release for irrigation from the downstream reservoir. When b is zero on the other hand, a represents the fraction of available storage that is allocated to irrigation. Note that the operating rule in (1) is a general release rule, defining the release for a target demand, irrigation in this case, as a function of the total available storage [*Oliveira and Loucks*, 1997]. The rule is implemented as a constraint in the annual optimization model, together with constraints on storage in each of the three reservoirs (see next section and Table 1). The combination of these various constraints results in an actual piecewise-linear operating rule, as illustrated in Figure 2: the actual release or allocation is either constrained by the linear release rule defined by (1) or by the amount of water available in the reservoirs.

[12] By means of these two decision variables, a and b, different conjunctive use strategies are obtained. For example, historical reservoir releases may be approximated by taking a = 0.47 and b = 990 (Figure 3). *Schoups et al.* [2006] found that by changing this historical rule to a = 0 and b = 1450, reductions in agricultural production during the recent drought could have been prevented by pumping more in wet years and storing extra reservoir water for irrigation during droughts.

[13] Two different objectives are considered in the long-term planning model. The first objective measures sustainability of irrigated agriculture and the second one measures the water losses spilled from the reservoirs to the ocean. Sustainability of alternative management strategies is evaluated in terms of the following three indices modified from *Cai et al.* [2002],

$$REL = \frac{1}{n}\sum_y IrrFrac_y \tag{2a}$$

$$RES = 1 - \frac{nfail}{n} \tag{2b}$$

$$IVUL = \min_y \left\{IrrFrac_y\right\} \tag{2c}$$

where REL is crop production reliability, RES is resiliency, and $IVUL$ is invulnerability or the opposite of vulnerability. $IrrFrac_y$ is the fraction of total irrigable land irrigated in year y, n is the total number of years considered, and $nfail$ was chosen as the number of consecutive years in the time series that irrigated acreage is smaller than 85% of total irrigable land. The value of 85% was selected as an appropriate cutoff value to distinguish between various operating rules. Sensitivity of the results to this value will be discussed later. Values for the sustainability indices vary between 0 and 1 with higher values indicating greater sustainability. They are combined into an overall weighted sustainability index [*Loucks*, 2000],

$$SUS = w_1 REL + w_2 RES + w_3 IVUL \tag{3}$$

Table 1. Objective Function and Constraints of the Annual Simulation-Optimization Model for Year y[a]

Constraint	Formulation	Simulation Models Used in Computation
Objective function	$Max \left\{ \sum_{m} \sum_{cr} CropAc_{y,m,cr}\left(CP_{y,cr} Y_{y,m,cr} + CS_{y,cr} - CC_{y,cr}\right) - \sum_{m} DC_{y,m} - \alpha \sum_{t} \sum_{k} Spill_{y,t,k} \right\}$	crop production model, groundwater model
Irrigable acreage	$0 \le \sum_{m} \sum_{cr} CropAc_{y,m,cr} \le CropAcTot$	
Pumping rate	$0 \le Pump_{y,t,w} \le PumpCap_{w}$	
Reservoir storage	$S_{\min,k} \le S_{y,t-1,k} + RO_{y,t,k} + (P_{y,t,k} - E_{y,t,k})\, A_{y,t,k} + f_c Q_{y,t,k-1} - Q_{y,t,k} - Spill_{y,t,k} - Q^{fix}_{y,t,k} \le S_{\max,k}$	reservoir model
Monthly release from downstream reservoir	$Q_{\min} \le \sum_{m} CW_{y,t,m} + \sum_{r} Q_{leak,y,t,r} \le Q_{\max}$	canal model
Annual release from downstream reservoir	$QA_{\min} \le \sum_{y} \left(\sum_{m} CW_{y,t,m} + \sum_{r} Q_{leak,y,t,r} \right) \le QA_{\max}$	canal model
Field-scale leaching fraction	$0 \le (1 - IrrigEff_{cr}) + \frac{DP_{y,m,cr}}{AW_{y,m,cr}} \le LCH_{\max}$	crop production model

[a]Indices are as follows: y is year, t is month, w is well, k is reservoir, m is module, cr is crop. A module is a water management unit in the district. There are 333 wells and 42 modules.

with values between 0 and 1, and the three weights w summing to 1. These weights reflect the decision maker's preference to each index. In the absence of any clear preferences, the weights were given equal values of 1/3, as in the work by *Cai et al.* [2002]. It is reasonable to assume that decision makers are equally concerned with all three aspects of the system's sustainability. Effects of the predefined weight values on the results are assessed after the optimization results are presented. Large values for *SUS* result from a policy that sustains agricultural production through extended droughts. Note that sustainability in terms of the risk of salinization of soil and groundwater resources is not included in (3). Instead, we assess salinization risk in a postoptimization phase, based on water table depths and aquifer head gradients near the coast, calculated by a regional groundwater model for the study area [*Schoups et al.*, 2005]. It is possible to explicitly incorporate environmental objectives into the optimization, as done by *Cai et al.* [2002] and *McPhee and Yeh* [2005].

[14] The second objective measures the water losses from the reservoirs to the ocean by minimizing total spills from the system using the following index,

$$SC = 1 - \sum_{y} Spill_y \Big/ \sum_{y} RA_y \tag{4}$$

where $Spill_y$ and RA_y are total annual spill and water allocation to irrigated agriculture respectively from the downstream reservoir. In other words, the spill control index *SC* measures total spills over a time horizon of n years expressed as a fraction of total reservoir releases to the district over the time horizon. Its value varies between

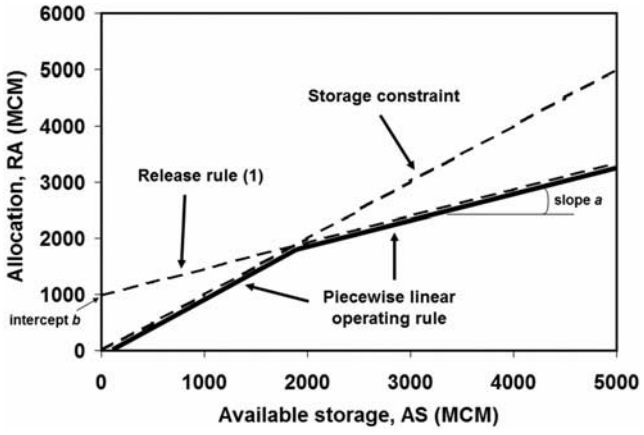

Figure 2. Piecewise linear operating rule consisting of (1) the linear release rule defined in equation (1) with slope a and intercept b and (2) storage constraint, limiting reservoir allocations to the available storage. MCM = 10^6 m^3.

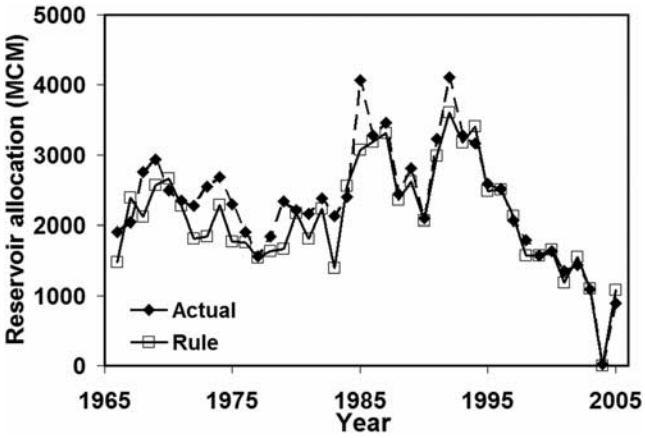

Figure 3. Time series of historical (''actual'') and empirically derived reservoir releases, using the linear release rule in (1) with slope a = 0.47 and intercept b = 990 $\times$ 10^6 m^3. Reservoir releases are annual water allocations to the district from the downstream reservoir, excluding urban water use (100 $\times$ 10^6 m^3). MCM = 10^6 m^3.

0 and 1, where 1 indicates no water losses and the absence of spills. Greater spills result in more water lost to the ocean and smaller values for *SC*. Although theoretically possible, in practice the value of *SC* does not become negative, i.e., over the long-term, spills are always smaller than reservoir allocation.

[15] The interannual optimization problem consisting of two objective functions, (3) and (4), and two decision variables, a and b in (1), was solved using an unconstrained global multiobjective optimization algorithm [*Vrugt et al.*, 2003]. Within a single optimization run, this algorithm generates a Pareto set of solutions that maximizes multiple objective functions. The algorithm relies on two key features. First, the fitness or optimality of candidate solutions is evaluated using the Pareto strength approach of *Zitzler and Thiele* [1999]. A score or fitness is assigned to each candidate point, based on its position in the multidimensional objective function space relative to other candidate points. A point (or solution) that performs better than another on all objectives is said to dominate the latter (concept of Pareto dominance), and its fitness score will depend on how many points it dominates. Second, the search strategy that generates new solutions is based on a Monte Carlo Markov chain (MCMC) sampler. In essence, new candidate points or solutions are randomly drawn from a multinormal distribution centered on the current points, and are accepted if they attain better fitness than the current points. Additional details are presented by *Vrugt et al.* [2003].

[16] In the following section we discuss the annual decision-making models that are nested within the interannual optimization framework. These annual models determine reservoir releases, spills, groundwater pumping rates and crop acreages.

3.2. Annual Optimization Model

[17] The purpose of the annual model is to determine annual decisions of surface water and groundwater use and cropping patterns in the district with the goal of maximizing total annual profit from agriculture (Figure 1). On the basis of available reservoir storage at the start of the year, decisions are made on reservoir allocations, groundwater pumping rates, and district-wide cropping patterns for the upcoming growing season. As shown in Figure 3, the annual surface water allocation for irrigation can be well described by the linear rule (1) with $a = 0.47$ and $b = 990$. In reality, cropping decisions are made by individual farmers within the district, whereas reservoir releases are managed by the National Water Commission (CNA). However, at the start of the growing season in September, a Hydraulic Committee, consisting of CNA representatives and local water managers, convenes to draft a valley-wide water plan. Even though farmers still have freedom to pick their crops, they do so within the constraints of the annual plan of the Hydraulic Committee. The annual optimization model mimics this situation by making profit-maximizing decisions on water use and cropping patterns as a single hypothetical planner for the entire district. As a consequence, the simulated crop mix is spatially uniform, which guarantees that profit is distributed equally throughout the district. *Schoups et al.* [2006] show that this formulation is able to reproduce irrigated acreages and water use decisions during the last 10 years.

[18] The annual model solves a nonlinear constrained optimization problem,

$$\begin{aligned} &\text{maximize} \quad OF_y(x) \\ &\text{subject to} \quad l_x \le x \le u_x \quad \text{and} \quad l_F \le F(x) \le u_F \end{aligned} \tag{5}$$

where OF_y is the annual objective function for year y (i.e., total annual agricultural profit in the district), which depends on the vector of decision variables $\boldsymbol{x}$ with lower bounds $\boldsymbol{l_x}$ and upper bounds $\boldsymbol{u_x}$, and $\boldsymbol{F}$ is a vector of smooth linear and nonlinear constraint functions also dependent on $\boldsymbol{x}$. Simulation models are used to calculate values for OF_y and $\boldsymbol{F}$ as a function of the decision variables $\boldsymbol{x}$. Table 1 summarizes the various constraints and simulation models used in the annual optimization model. The crop production model calculates crop yields as a function of the amount and the salinity of the applied irrigation water. The canal model routes water and salts through the main irrigation canals, and accounts for diversions from and pumping into the canals. The reservoir model consists of water balance equations for each of the three reservoirs on the Yaqui River to compute monthly reservoir storages as a function of inflows and outflows (runoff, precipitation, evaporation, releases). Finally, a regional groundwater model of the alluvial aquifer is used to calculate the impact of irrigation and pumping on shallow and deep groundwater heads. As opposed to the study by *Schoups et al.* [2006], here the groundwater model is not part of the annual optimization but instead is run annually to update hydraulic heads, as shown in Figure 1. Pumping costs are calculated based on simulated heads from the regional groundwater model at the beginning of the year, with monthly in-well drawdown corrections during the year.

[19] Decision variables include (1) monthly reservoir releases from the two upstream reservoirs on the Yaqui River, (2) annual groundwater pumping in 42 modules (management units within the district) and into three main irrigation canals within the district, and (3) seasonal district-wide acreages for 10 crops. Cropping patterns are assumed to be uniform within the district, and module-scale groundwater pumping is downscaled to individual wells based on well pumping capacities. Monthly spills from each reservoir are also included as decision variables, and are only allowed to occur when reservoirs are at full capacity. This is achieved by including the total volume of reservoir spills as an extra term in the objective function, as shown in Table 1. Note that the spill term has a negative sign, such that spills are minimized. The net effect is that spills only occur when necessary, i.e., to avoid an infeasible problem: when the reservoir is at full capacity spills are the only option to keep reservoir storage at or below its upper limit. The spill term in Table 1 is multiplied by a scaling factor whose value is chosen sufficiently small to prevent the spill term from dominating the profit-maximizing objective.

[20] Monthly releases from the downstream reservoir (Oviachic) are calculated as a function of crop water demand and groundwater use, and are implemented as constraints. Additional constraints are specified for irrigable acreage, pumping capacities, reservoir storages, annual release from the downstream reservoir by (1), and field-scale leaching from irrigation (Table 1). The integrated annual simulation-optimization model includes a large number of

Table 2. Parameters of the Management Model[a]

Parameter Class	Description[b]
Costs	energy cost (1); district annual fixed costs (2)
Crops	crop prices (3); crop subsidy (3); crop production costs (3); potential crop yield (3); water and salt stress (4) parameters for each crop; irrigation efficiency (2); crop irrigation schedule (2)
Modules	module area (2); module water distribution efficiency (2)
Reservoirs	parameters of the area-storage relationships (6); precipitation (6) and evaporation[c] (6) depths for each reservoir; monthly run-off into each reservoir (6), assumed known for each sequential water year
Canals	for each reach: length; width; slope and roughness parameters; conductivity and thickness of the canal bed material (2,5)
Groundwater	monthly pump capacity (2); well elevation (5); aquifer transmissivity (5,7); pump efficiency (2); groundwater salinity (2); horizontal and vertical hydraulic conductivities; groundwater storage parameters; drainage parameters (5, 7)

[a]Various data sources were used to estimate parameter values, as indicated.

[b]Data sources are as follows: 1, Comision Federal de Electricidad; 2, Yaqui Irrigation District; 3, Sagarpa; 4, *Maas* [1990]; 5, *Addams* [2004]; 6, Comisión Nacional del Agua; 7, *Schoups et al.* [2005].

[c]Average reservoir evaporation rates are used in the model; variability in evaporation is not considered.

parameters, related to energy costs for pumping, crop-specific parameters, module-based parameters, reservoir parameters, well parameters, and parameters for the groundwater model (Table 2). The constrained nonlinear optimization problem represented by (5) is solved using the large-scale gradient-based solver SNOPT [*Gill et al.*, 2002]. We refer to *Schoups et al.* [2006] for a detailed description of the annual optimization model and a comparison to historical management.

3.3. Input Parameters

[21] A large number of parameters related to surface water, groundwater, and agronomics must be specified in the integrated water management model (Table 2). A major source of uncertainty is the future evolution of crop prices and production costs, especially in view of large year-to-year variations in the historical values of these parameters. For example, the economic profitability of many crops may change dramatically over the short term, making it difficult to predict future changes or to select a representative year for extrapolation. To account for the average behavior, we used average crop prices and production costs from the last 10 years. These average values were then held constant for the entire prediction period (20–30 years). The assumption is that crop profitability will not change significantly from average conditions. Ten crops were simulated, including corn, wheat, cotton, vegetables, alfalfa, and citrus, and lower and upper limits on crop acreages were determined based on historical conditions. Each simulation starts at the beginning of October 2005, and runs for either 20 years or 30 years into the future. Initial values for water storage in the surface reservoirs were based on actual conditions in September 2005. Initial hydraulic heads in 2005 were obtained by prediction with the groundwater model starting from measured heads in 1995. Monthly Yaqui river runoff is specified for each reservoir based on either historical data for the past 20 years (1986–2005) or synthetic data (30 year sequences) generated by the stochastic streamflow model, which is described in the next section. The historical period of 1986–2005 was selected because it incorporates the full range of observed streamflow variability over the entire historical record. Thirty years was selected for the stochastic record length, because it is a standard time horizon for planning purposes.

[22] Although significant uncertainty exists about future crop prices and production costs, this source of uncertainty is not considered here. Instead, crop prices and production costs are treated as deterministic and constant parameters. In reality, changes in crop profitability may eventually result in permanent shifts in the types of crops grown in the Valley. Handling these effects requires numerous assumptions and is beyond the scope of the current study.

3.4. Computational Considerations

[23] The optimization problem discussed above constitutes a computational challenge in terms of required computing memory and processing speed, due to the long-term nature of the problem (20–30 years) and due to its stochastic nature. In this paper, the computational burden is significantly reduced by (1) solving the problem more efficiently using a hierarchical approach and (2) studying the stochasticity of the problem due to uncertainty in streamflow after applying interannual optimization using Monte Carlo simulation. First, the hierarchical approach effectively breaks up the problem into a number of smaller, annual optimization subproblems, which are linked together by an interannual optimization formulation over the entire period. The interannual model contains only a limited number of decision variables, and is therefore computationally manageable (Figure 1). Second, the original stochastic optimization problem is converted into a deterministic one, by first identifying optimal conjunctive use rules for a 20 year historical streamflow record, followed by an assessment of the reliability of these rules using Monte Carlo simulation based on 100 30 year synthetic streamflow records.

[24] The resulting computational burden becomes manageable. The hierarchical optimization and simulations for the 20 year historical streamflow record were performed on an Intel Xeon 3.6 GHz workstation with 4 Gb of RAM. Each annual optimization followed by a 1 year groundwater simulation (one cycle in the annual loop of Figure 1) took on average 20 s. Therefore a 20 year optimization simulation run for a given operating rule, i.e., fixed values for slope and intercept parameters a and b in (1), took about 7 minutes (20 cycles in the annual loop of Figure 1). The multiobjective optimization algorithm generated 800 realizations of parameters a and b, resulting in a total runtime of approximately 90 hours. With regard to software, the computations were performed by linking Excel/Visual Basic, which serves as a user interface for the model, with (1) the multiobjective optimization algorithm written in Matlab [*Vrugt et al.*, 2003], and (2) the simulation models [*Schoups et al.*, 2006] and the gradient-based optimization algorithm [*Gill et al.*, 2002] using Fortran-compiled dynamic link libraries.

[25] For the postoptimization Monte Carlo analysis, each of the 31 Pareto solutions identified by the multiobjective optimization were tested using 100 synthetic runoff records, each 30 years long. This resulted in a total of 93,000 annual optimizations and groundwater model runs, and a total computing time of 21.5 days. However, the Monte Carlo

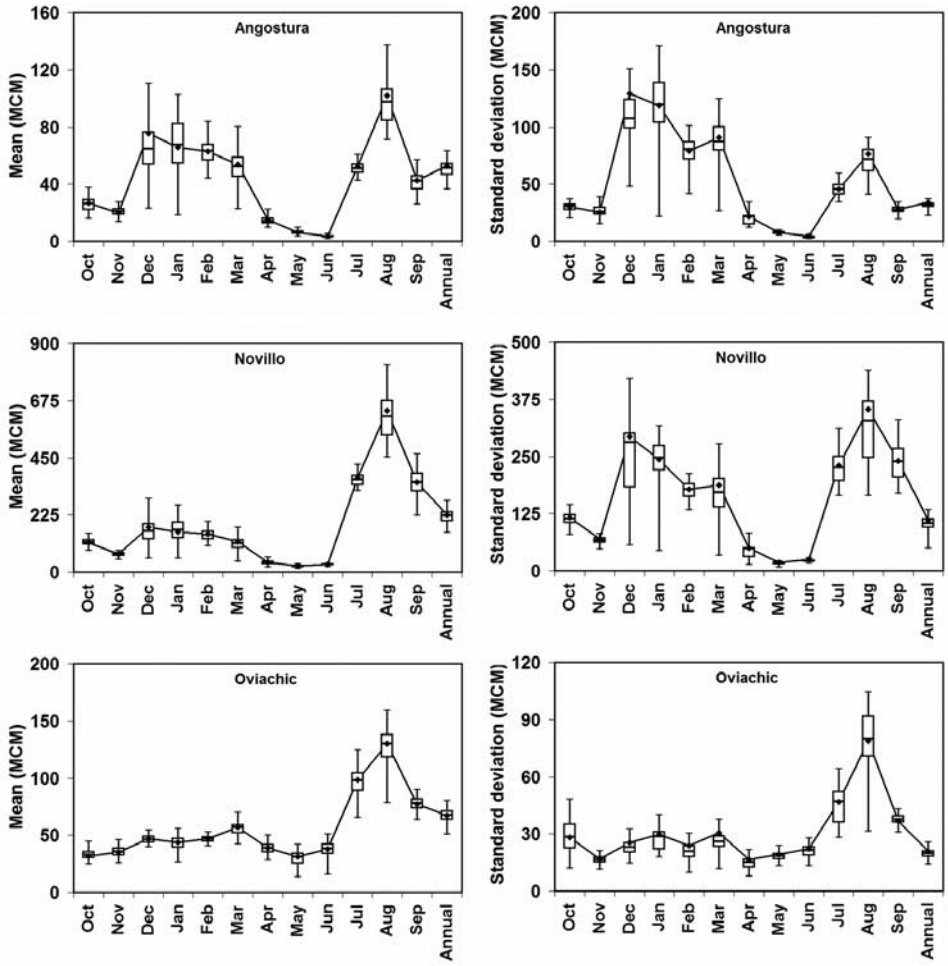

Figure 4. Comparison of generated (box plots) and observed (lines) streamflow (left) means and (right) standard deviations. For display purposes, annual streamflow values were divided by 10. MCM = 10^6 m^3.

calculations were performed in parallel on four Xeon workstations, resulting in an actual runtime of about 5.4 days.

4. Stochastic Streamflow Generation

[26] Best future management strategies critically depend on how much runoff will occur in the Yaqui river system. In view of the uncertainty of future runoff, a stochastic time series model of Yaqui river flows was used to generate a large number of equally probable streamflow realizations. The optimization problem was then solved for each of these realizations, and best management statistics were derived based on all the optimization results. Thirty year monthly streamflow time series for each of the three reservoirs on the Yaqui river (Angostura, Novillo, and Oviachic) were generated with the method of *Srinivas and Srinivasan* [2005], called the hybrid moving block bootstrap multisite model (HMM). The method combines the strengths of parametric and nonparametric approaches to time series analysis, i.e., it is simple and requires no assumptions about the shape of the pdfs (nonparametric attribute) and as opposed to simple bootstrapping it generates flows that lie outside the minima and maxima of the historic record (parametric attribute). The goal is to generate synthetic time series of monthly streamflow at each of the three reservoirs such that both univariate (mean, standard deviation, autocorrelations) and multivariate (cross correlations) statistics of the observed streamflow data are preserved. The algorithm generates time series of monthly streamflow that mimic both short-term and seasonal characteristics, and long-term and cross-site correlations of the observed streamflows. A block length of 4 years was selected to account for multiyear correlations in the streamflow record, which is necessary to simulate longer drought periods. A further advantage of the nonparametric part of the algorithm is that no assumptions are made about the normality of the residuals. A detailed description of the different steps of the algorithm is given by *Srinivas and Srinivasan* [2005].

[27] Forty years of monthly streamflow data at each of the three reservoirs were used to calibrate the HMM model. The three sets of streamflow data were corrected for upstream reservoir releases such that they represented natural flows only. Observed streamflow data were used to estimate the model parameters (means, standard deviations, and lag 1 autocorrelation coefficients for each reservoir). The algorithm was then used to generate 100 equally probable 30 year realizations of monthly streamflow time series at each of the three reservoirs. These numbers were used in the

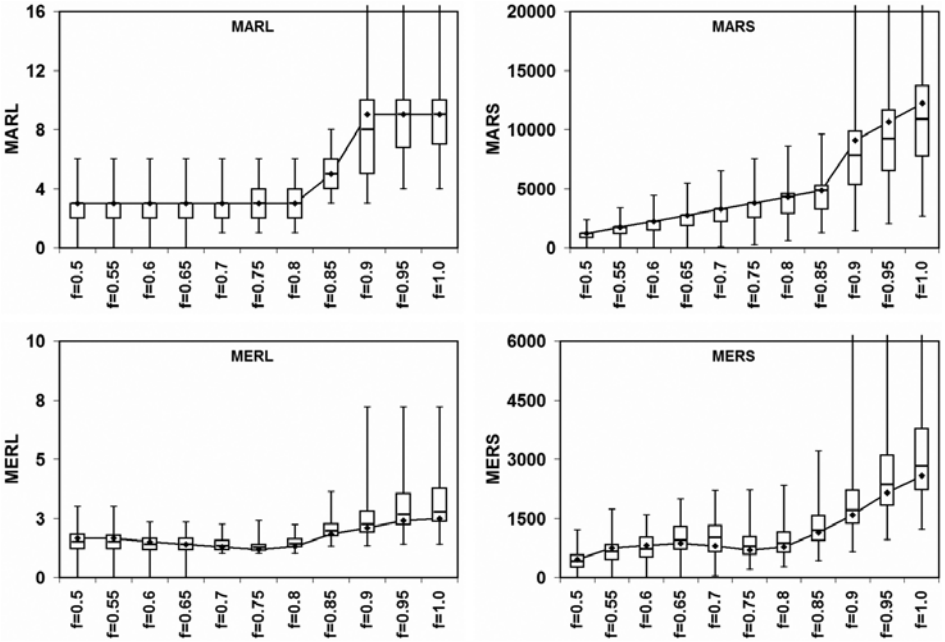

Figure 5. Comparison of generated (box plots) and observed (lines) drought characteristics of streamflow, as defined in (6): maximum run length (MARL), maximum run sum (MARS), mean run length (MERL), and mean run sum (MERS).

optimization model to describe natural streamflow, and were augmented with releases from upstream reservoirs (see Table 1 for the reservoir water balance). It should be noted that the generated streamflows do not account for possible future effects of climate change that would result in fundamental changes in the flow statistics.

[28] Results of the stochastic streamflow generation algorithm are evaluated by comparing statistics of the generated streamflow records to statistics of the observed streamflows during the last 40 years. This is done for both annual and monthly timescales, and for inflows into the three reservoirs on the Yaqui River (Angostura, Novillo, and Ovaichic). Figure 4 shows mean and standard deviations of observed monthly and annual streamflows, as well as box plots of the corresponding simulated streamflows. The seasonal pattern of streamflow is obvious with recorded peaks during the Monsoon season (July–September). Standard deviations are proportional to mean flows, reflecting greater interannual variation in wetter months. It can be seen that the simulated streamflow values capture the seasonality of the observations. Short-term (within year) autocorrelations and cross correlations were also well reproduced by the model (not shown). Figure 5 shows how well the generated streamflow realizations mimic observed drought characteristics of the historical 40 year record. Four different drought indicators are plotted, namely the maximum (drought) run length (MARL) and the mean (drought) run length (MERL), and the maximum run sum (MARS) and mean run sum (MERS), as presented by *Srinivas and Srinivasan* [2005]. For a given streamflow record, these are calculated as follows,

$$MARL = \max\{dl_1, \ldots, dl_m\} \tag{6a}$$

$$MARS = \max\{s_1, \ldots, s_m\} \tag{6b}$$

$$MERL = \frac{1}{m}\sum_{i=1}^{m} dl_i \tag{6c}$$

$$MERS = \frac{1}{m}\sum_{i=1}^{m} s_i \tag{6d}$$

where dl_i is the length in years of the ith drought, s_i is total deficit of the ith drought, and m is the number of droughts in the record. A drought in this context is defined as a continuous period during which flows into each of the reservoirs are below their respective predefined truncation levels. In Figure 5, truncation levels are taken as specified fractions f of the mean annual streamflow. Drought deficit s_i measures the magnitude by which flows are below the truncation levels, by taking the difference between the actual flows and the truncation levels and summing the result over all reservoirs. The model does a reasonable job of reproducing the drought characteristics of the historical record. More severe droughts, corresponding to small f values, are better preserved than less severe ones (larger f). Nevertheless, the model reproduces the recent 8 year drought (MARL = 8 for $f = 0.9–1.0$), but also produces realizations that contain droughts that are both longer and shorter than this historical drought.

5. Results and Discussion

[29] Discussion of the results is divided into two main parts. First, optimization results identifying optimal operating rules for the historical runoff time series are discussed. This is followed by a postoptimization evaluation of the performance of the optimal operating rules identified in the first part, based on synthetic streamflow realizations.

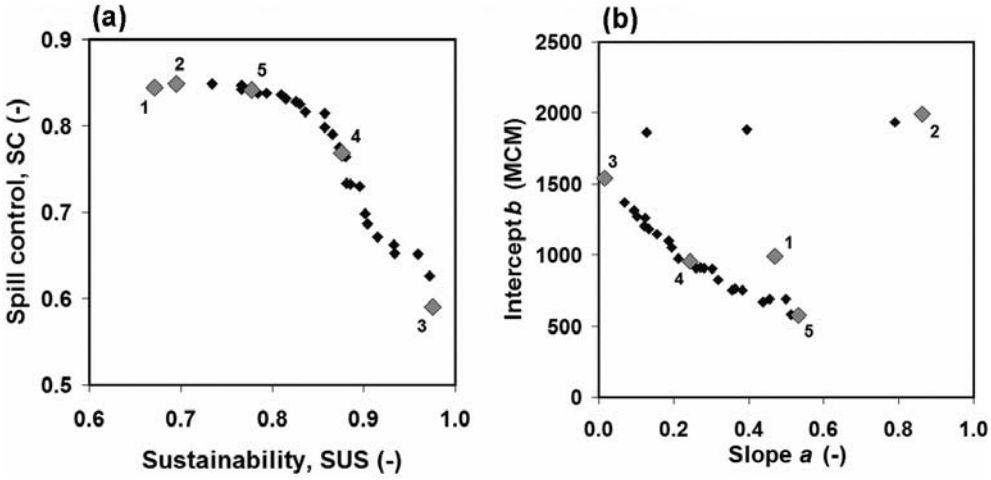

Figure 6. (a) Pareto trade-off curve between sustainability and spill control, as measured by the indices in (3) and (4), generated by the multiobjective optimization and (b) the corresponding slopes and intercepts of the Pareto optimal operating rules. The historical streamflow record for the last 20 years (1986–2005) was used (Figure 3). Each solid diamond corresponds to a particular operating rule of the form (1). Shaded diamonds indicate rules of special interest, corresponding to numbers in Table 3.

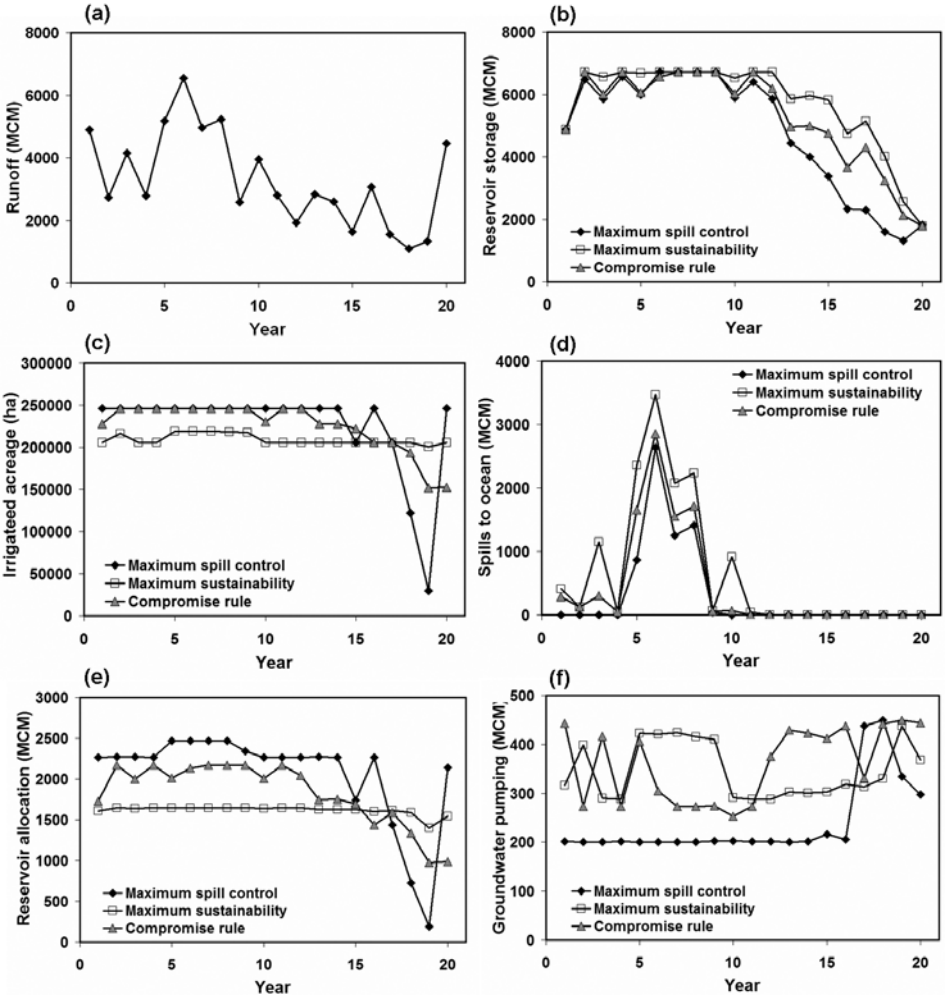

Figure 7. Detailed results for selected operating rules using (a) the historical streamflow record, showing time series of (b) reservoir storage, (c) irrigated acreage, (d) spills to the ocean, (e) reservoir allocation to the district, and (f) groundwater pumping for irrigation. Results are shown for three rules, corresponding to numbers in Table 3 and Figure 6. MCM = 10^6 m^3.

Table 3. Selected Conjunctive Use Operating Rules, Specifying Annual Reservoir Allocation RA_y as a Function of Available Reservoir Storage AS_y at the Start of the Year Using a Linear Operating Rule, $RA_y = a \times AS_y + b$[a]

Index	Slope a	Intercept b	Description
1	0.47	990	historical rule
2	0.86	1989	maximum spill control
3	0.02	1542	maximum sustainability
4	0.24	953	compromise rule
5	0.53	577	near-maximum spill control

[a]Indices correspond to numbers in Figures 6 and 8.

5.1. Optimal Historical Operating Rules for Agricultural Sustainability and Spill Control

[30] Figures 6 and 7 show results of the interannual optimization using the historical runoff time series. The aim is to find operating rules of the form (1) that both maximize sustainability of agricultural production during droughts and minimize spills during wet periods. The multiobjective optimization identified a Pareto trade-off curve (Figure 6) between maintaining agricultural production during droughts, as measured by the sustainability index (3), and minimizing spills during wet periods of increased runoff, as quantified by the spill control index (4). Figure 6a indicates that for the historical time series it is not possible to maximize the two conflicting objectives both at the same time. Figure 6b shows how the optimal operating rule varies as one moves along the Pareto curve. For discussion, we selected five different operating rules, as summarized in Table 3 and shown by numbers in Figure 6. These include (1) the historical rule, (2) the minimum spill rule, (3) the maximum sustainability rule, (4) a compromise rule that yields intermediate levels of spills and sustainability, and (5) a rule that results in near-optimal spill control. Time series of historical runoff, reservoir storage, allocation, groundwater pumping, irrigated acreage, and spills for three of these rules are shown in Figure 7.

[31] When the emphasis is entirely on agricultural sustainability without consideration of spills (rule 3), the optimal operating rule that maintains agricultural production during droughts is to allocate annual reservoir water to irrigation in the district equal to 1542×10^6 m^3 (Figure 6b and Table 3). Since the optimal slope a is almost zero in this case (Figure 6b and Table 3), this allocation is more or less independent of how much water is available in the reservoir at the start of the growing season (Figure 7e). The idea behind this rule is to limit releases from the reservoir during wet years, such that more water is available during droughts. With the upper limit on reservoir allocation, the remaining crop water demand is satisfied by groundwater pumping at a rate of $300–400 \times 10^6$ m^3 every year (Figure 7f). Note that the maximum annual pumping capacity is 450×10^6 m^3. This operating rule results in a maximum sustainability index of 0.98 for the historical record (Figure 6a). There are two issues with using this rule however. First, due to the imposed limit on reservoir allocation of about 1600×10^6 m^3 and a maximum pumping capacity of 450×10^6 m^3, crop production during wet years is limited to winter crops to allow continued production during droughts (Figure 7c). Second, an obvious drawback is that by limiting reservoir allocation for irrigation, too much water is being stored in the reservoirs (Figure 7b). This excess storage results in significant spills during wet periods (Figure 7d), as also evidenced by the low value of the spill control index for this rule, namely 0.60 (Figure 6a). This means that according to (4), total spills constitute 40% of all irrigation water releases during the 20 year historical period. In other words, the operating rule that maximizes agricultural sustainability prescribes storing water in the reservoirs for future droughts, which leads to large losses and spills to the ocean.

[32] An alternative is to minimize spills without much concern for agricultural production. The operating rule that minimizes spills (rule 2 in Table 3 and Figure 6) results in a spill control value of 0.85 and a sustainability index of 0.70 (Figure 6a). Therefore, using historical runoff, spills cannot be avoided no matter which operating rule is used. The reason for this is that there is an upper limit on irrigated acreage and hence crop water demand within the district. If runoff during wet years is beyond the value that can be physically used for irrigation in the district, then this additional water has to be disposed of by spilling to the ocean. There is the possibility of growing second crops during the summers, thereby essentially doubling irrigated acreage and greatly increasing crop water demand during wet years. However, under current economic conditions corn is the only viable summer crop, which has been limited to about 40,000 ha (20% of irrigable land) based on historical conditions. Before 1995 soybean was a major summer crop until a widespread whitefly infestation in 1995 reduced soybean production in the Yaqui Valley to essentially zero [*Naylor et al.*, 2001]. Therefore the absence of a viable summer crop such as soybeans increases the risk of spills. For example, simulation results indicated (Figure 7d) that spills were unavoidable during years 5–8 due to very large runoff volumes (Figure 7a). Since in our analysis we are using the historical runoff record for the period 1986–2005, the same runoff for years 5–8 occurred historically during 1990–1993. There were actual spills in the system during that time, namely in 1991 and 1992 (J. L. Minjares, Comisión Nacional del Agua, Cuidad Obregón, Mexico, personal communication, 2005). However, actual spills amounted to 3558×10^6 m^3, whereas simulated spills during years 5–8 totaled 6213×10^6 m^3. The difference (2616×10^6 m^3) corresponds to a difference in actual (1990–1993) and simulated (years 5–8) reservoir allocation which amounts to 2832×10^6 m^3. The greater actual allocation was largely due to an annual soybean production of almost 100,000 ha compared to none in the model, because soybeans are no longer a viable crop. Therefore, after correcting for the differences in simulated and actual reservoir allocations, the simulated spills using the minimum spill rule correspond quite well with the actual spills during 1990–1993.

[33] As expected, the linear operating rule that maximizes spill control has both a large slope (a = 0.86) and a large intercept (b = 1989×10^6 m^3) to maximize reservoir releases to the district within the limits of irrigated acreage and summer crop profitability (Table 3 and Figure 6b). Because of these limits, rules with larger slopes and intercepts do not produce smaller spills. As a matter of fact, Figure 6 suggests that there is a wide range of operating rules that all result in a similar level of spill control, as illustrated by the results for the historical rule (rule 1 in

Table 4. Effect of Cutoff Value for Irrigated Acreage on the Resiliency Index *RES* and the Overall Sustainability Index *SUS*, Equation (3)[a]

Index	Statistic	Cutoff Value 75%	85%	95%
RES	average	0.98	0.96	0.92
RES	standard deviation	0.04	0.06	0.09
RES	minimum	0.77	0.67	0.57
RES	maximum	1.00	1.00	1.00
SUS	average	0.94	0.93	0.92
SUS	standard deviation	0.08	0.09	0.10
SUS	minimum	0.67	0.63	0.61
SUS	maximum	1.09	1.09	1.09

[a]For example, a cutoff of 85% means that a failure is recorded when irrigated acreage in a certain year is less than 85% of total irrigable acreage. Statistics are calculated for *SUS* and *RES* over all realizations and all Pareto optimal operating rules.

Table 3 and Figure 6) and alternative rule 5. Consequently, the entire variation of the Pareto trade-off curve is sampled by moving from rule 3 (maximum sustainability) to rule 5 (near-optimal spill control. Figure 6b shows that this corresponds to decreasing intercepts and increasing slopes.

[34] Given the trade-off between the sustainability and spill control objectives, it is useful to examine compromise solutions in between the two extremes discussed so far. The Pareto trade-off curve in Figure 6 contains all the information to select an alternative management strategy depending on the relative preference that is given to the two objectives. Although many solutions may be selected, we discuss here one potentially useful alternative, rule 4 or the compromise rule (Table 3 and Figure 6). This solution provides intermediate spill control of 0.77, compared to the maximum value of 0.85, and at the same time it also sustains agricultural production during drought periods, as shown by the sustainability index of 0.88 (compared to the maximum value of 0.98). The corresponding reservoir operating rule is defined by an intermediate slope and intercept (Table 3 and Figure 6b). It allocates water more dynamically than the sustainability maximizing rule, which was independent of available storage, but more conservatively than the spill-minimizing rule, resulting in intermediate levels of reservoir storage, irrigated acreage, and spills (Figure 7).

[35] Finally, Table 4 shows the effect that the cutoff irrigated acreage value has on calculated resiliency *RES* and sustainability *SUS* indices. Remember in (2b) that this cutoff was taken as 85%, i.e., a failure is recorded when the irrigated acreage is smaller than 85% of total irrigable land. As expected, the *RES* index is sensitive to the cutoff value with larger cutoff values resulting in more failures and a smaller value for *RES*, see (2b). Since the other two indices that make up the sustainability index *SUS* by definition do not depend on the cutoff value, *SUS* values are less sensitive to the cutoff value (Table 4).

[36] In the following sections, runoff uncertainty is quantified using the stochastic streamflow model, and performance of the alternative management strategies that were discussed here is evaluated for this uncertainty.

5.2. Postoptimization Evaluation of Performance of Optimal Operating Rules Under Streamflow Uncertainty

[37] The purpose of this section is to evaluate the performance of the Pareto alternative management strategies that were identified in the previous section. This is done by means of a Monte Carlo analysis, whereby the model was run for each of one hundred 30 year streamflow realizations that were generated with the stochastic streamflow model in section 4. The Monte Carlo simulation was repeated for each of the 31 Pareto solutions in Figure 4a, each corresponding to a particular linear operating rule (Figure 6b). Each 30 year model run consisted of 30 consecutive annual optimizations without running the interannual optimization (Figure 1), since the operating rules were specified in advance. Hence the Monte Carlo analysis consisted of 100 realizations $\times$ 30 years $\times$ 31 Pareto solutions = 93,000 annual optimizations and groundwater model runs (Figure 1).

[38] Figure 8 presents trade-offs between corresponding percentiles of the two objective functions, i.e., spill control, *SC*, and agricultural sustainability, *SUS*. These curves are similar to the deterministic results in Figure 6, except that now different trade-off curves are obtained for each percentile. For example, the 50% percentile curve indicates the trade-off between the medians of *SC* and *SUS*. Note that this median curve is shifted toward larger *SUS* values compared to results for the historical 20 year streamflow record (Figure 6a). This is likely due to the greater weight given to the recent drought in the 20 year historical record, compared to the generated streamflow time series, which are based on a resampling of the entire 40 year historical record. Nevertheless, the relative behavior of the different selected operating rules in Figure 8 is the same as in Figure 6a. In other words, spill control percentiles for the spill-minimizing rule (rule 2) in Table 3 are greater than those for all other rules. Therefore the results of the postoptimization Monte Carlo analysis confirm the performance of selected rules in the multiobjective optimization, suggesting that our approach of first identifying optimal rules based on the 20 year historical record was valid.

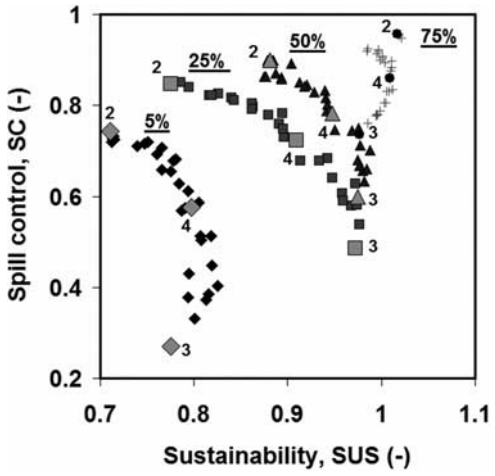

Figure 8. Postoptimization Pareto trade-off curves between corresponding percentiles of the sustainability and spill control indices for 100 realizations of 30 year synthetic streamflow records. Results are shown for the 5% (diamonds), 25% (squares), 50% (triangles), and 75% (crosses) percentiles. Each solid diamond corresponds to a particular operating rule of the form (1). Shaded diamonds indicate rules of special interest, corresponding to numbers in Table 3. The 50% percentiles correspond to the median SC and SUS values.

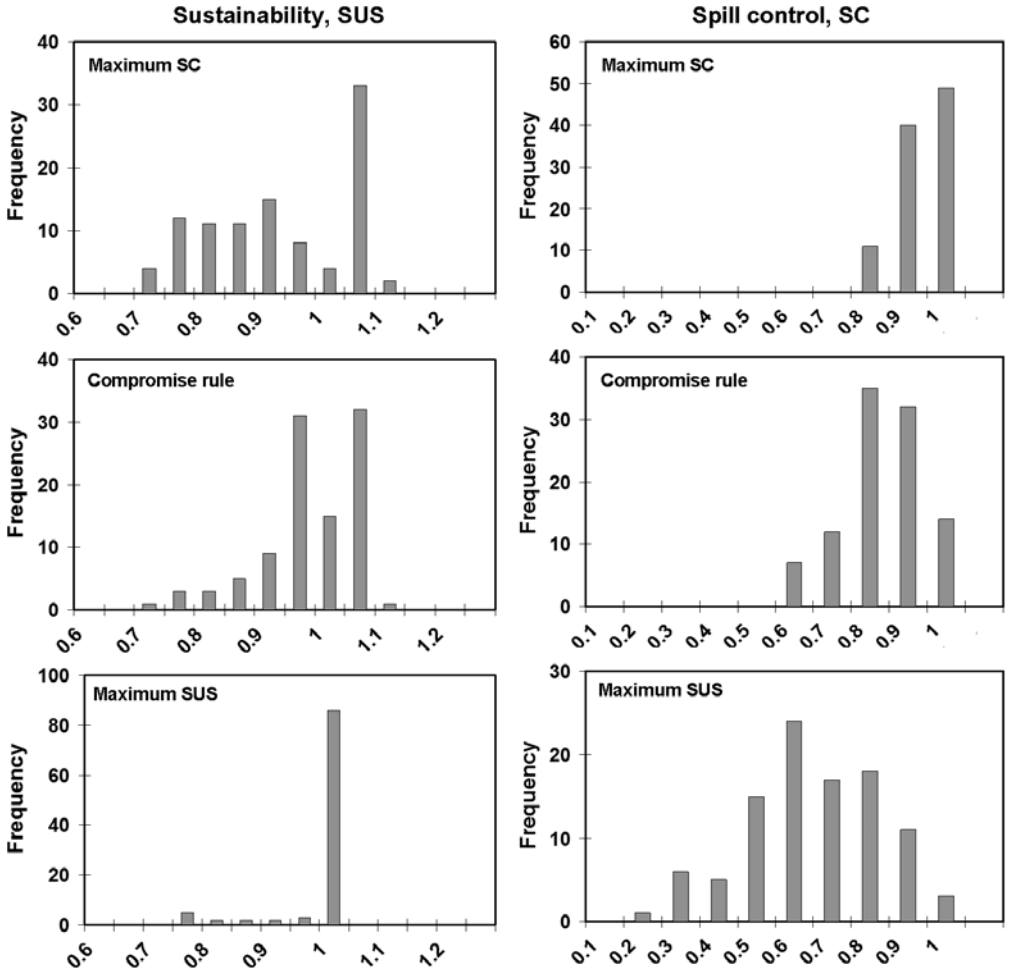

Figure 9. Postoptimization histograms of the sustainability and spill control indices for 100 realizations of 30 year synthetic streamflow records and three selected operating rules from Table 3: maximum spill control (rule 2), compromise rule (rule 3), and maximum sustainability (rule 4).

[39] Figure 9 shows histograms of the sustainability and spill control indices for each of the one hundred 30 year streamflow realizations, and for three selected operating rules. The spill-minimizing rule results in large irrigated acreages during wet periods, as shown by a peak in its *SUS* histogram near 1. Values for *SUS* greater than 1 indicate that summer crops are grown (up to an upper limit of 40,000 ha) in addition to a full winter crop acreage. However, this rule also yields a long tail of smaller *SUS* values, confirming that not enough water is available to sustain agricultural production during droughts. The *SUS* histogram for the sustainability-maximizing rule on the other hand is entirely centered on 1 with a very small low-end tail, indicating that this rule creates maximum protection against droughts. As discussed earlier, this is possible by pumping more groundwater during wet periods, such that more surface water is available during droughts. Note however, that some small *SUS* values are unavoidable during extreme droughts. The drawbacks of this strategy are the absence of summer crops in wet periods, and many spills, as also shown in Figure 9 by the wide histogram for spill control. The compromise rule (Table 3) yields intermediate histograms for both *SUS* and *SC*. The *SUS* histogram has a smaller low-end tail compared to the spills-minimizing rule and the *SC* histogram is shifted toward larger *SC* values compared to the sustainability maximizing rule.

[40] These results can be used by water managers to identify an optimal operating rule that gives desired levels of sustainability and spill control. Although a particular compromise rule was selected here, many different management strategies could be selected depending on end user preference. For example, the Pareto trade-off curves in Figure 8 may aid in negotiations to reach a compromise solution for water management in the Yaqui Valley. The actual final solution will depend on the preferences of the different parties involved (farmers and water managers), in terms of short-term versus long-term perspective and risk aversion.

[41] Finally, Table 5 shows the effects of three selected rules on water table elevations and groundwater head gradients near the coast. Shallow water tables pose a risk of soil salinization by capillary rise and subsequent evaporation, whereas landward groundwater head gradients may result in seawater intrusion and groundwater salinization. Since the compromise and sustainability maximizing rules rely to a greater extent on groundwater pumping, they result in lower water tables (Table 5). The trend in the coastal groundwater head gradient is less clear, but none of the rules apparently pose a risk of seawater intrusion, as suggested by

Table 5. Minimum Water Table Depths and Coastal Groundwater Head Differences for Selected Operating Rules[a]

Index	Rule	Minimum Water Table Depth, m	Minimum Groundwater Head Difference, m
2	maximum spill control	1.45	0.15
3	maximum sustainability	1.66	0.17
4	compromise rule	1.53	0.12

[a]A positive groundwater head difference indicates that groundwater flows toward the coast (no seawater intrusion). Indices correspond to numbers in Figures 6 and 8.

positive values indicating groundwater discharge to the sea. In an earlier study [*Schoups et al.*, 2006] we found that seawater intrusion only becomes an issue when additional regional well capacity is installed beyond what is currently available.

5.3. Discussion

[42] One potential drawback of our method, i.e., deterministic optimization using a long historical record followed by Monte Carlo testing of the resulting optimal rules, is that the rules that were identified as (Pareto) optimal in the interannual optimization are not necessarily optimal for the streamflow realizations used in the Monte Carlo analysis. In order to find optimal rules under uncertainty one would need to solve the optimization problem for each of the streamflow realizations (as in the work of *Young* [1967]) or find an optimal strategy for all synthetic streamflow realizations at once. In either case, the computational burden would be significantly larger. We instead test the performance and reliability of the Pareto optimal rules on a large number of streamflow realizations. The advantage is a significant reduction in computational load. In addition, since the Pareto set of solutions spans a wide range of possible strategies (slopes from 0 to 0.8, intercepts from 500 to $2{,}000 \times 10^6$ m^3, see Figure 6), the Monte Carlo analysis is more robust than when a single optimal solution would be tested.

[43] Another potential drawback is that, while in reality intra-annual decisions are made under uncertainty, the model finds optimal monthly allocations assuming that the monthly streamflows for the entire year are known before the fact. This may lead to optimistic results compared to what is possible in reality. However, we believe that this effect is limited because (1) intra-annual decisions are to a large extent constrained by the annual allocation, which is determined as a function of available storage at the start of the year through the linear operating rule (1), and (2) in reality actual monthly allocations may be adjusted to adapt to actual conditions throughout the year.

[44] The interannual optimization may be too severely constrained by the linear operating rule in (1). A more flexible rule, e.g., a nonlinear or piecewise linear rule, could perhaps partially alleviate the trade-off between spill control and sustainability in Figure 6. This would make it possible to identify two separate rules (with different slopes and intercepts) for droughts and wet periods. By specifying a linear rule it was possible to keep the number of decision variables in the interannual optimization model to a minimum, but it may have limited the flexibility of the formulation.

[45] In (3) it was assumed that the decision maker attaches equal importance to the three aspects of the system's sustainability by a priori setting values for the weights, w, equal to 1/3. Table 6 illustrates the effect of the weight values on the results. It shows statistics for the three sustainability indices (REL, RES, IVUL), computed from the results for all 100 realizations and all 31 Pareto solutions. We find that (1) IVUL has the greatest variability, and thus is the best index to separate good from bad management and (2) there is significant correlation between RES and IVUL, indicating that these two indices are somewhat complementary. These results suggest that for the Yaqui Valley IVUL is the most important index to include, and that the other indices and their weights have a secondary effect.

6. Summary and Conclusions

[46] We presented a methodology to aid in identifying optimal conjunctive use rules for water management in irrigated agriculture, with a case study in the Yaqui Valley, Mexico; a region that historically has produced 40% of Mexican wheat. Operating rules were parameterized as linear relations between initial reservoir storage at the start of the growing season and maximum annual reservoir release. Each rule was characterized by a slope and intercept. A hierarchical optimization approach was used, consisting of multiobjective long-term optimization for spill control and agricultural sustainability coupled to annual profit maximization using a gradient-based algorithm. Optimization results using a 20 year historical streamflow record yielded a Pareto trade-off curve between providing minimal spills during wet periods and sustaining agricultural production during droughts. In general, operating rules with near-zero slopes and intercepts around 1500×10^6 m^3 resulted in a maximum level of sustainability by promoting groundwater use during wet periods. By gradually increasing the slope of the linear operating rule, one moves along the Pareto front from maximum sustainability to minimum spills. In between these two end-member rules, one finds a set of compromise rules that provide intermediate levels of sustainability and spills.

[47] The second objective of our study was to evaluate the performance of these operating rules under streamflow uncertainty. A stochastic streamflow model for the Yaqui River was used to generate one hundred 30 year streamflow

Table 6. Statistics of the Three Sustainability Indices Defined in (2), Computed From All Results (100 Streamflow Realizations and 31 Pareto Optimal Solutions)

Index	Average	Minimum	Maximum	Coefficient of Variation	Correlation Coefficient *REL*	*RES*	*IVUL*
REL	1.05	0.93	1.14	0.04	1.00	0.43	0.31
RES	0.96	0.67	1.00	0.06	0.43	1.00	0.77
IVUL	0.78	0.20	1.14	0.26	0.31	0.77	1.00

realizations, based on a historical 40 year record of monthly streamflows at each of the three reservoirs. The model preserves observed means, standard deviations, and correlations in time and space. The performance of 31 Pareto alternative management strategies was then evaluated using a Monte Carlo analysis, wherein the optimization model was run for each of one hundred 30 year streamflow realizations. Results confirmed the performance of selected operating rules in the multiobjective optimization using the historical streamflow record, suggesting that our approach of first identifying optimal rules based on the 20 year historical record was valid. We quantified the effects of streamflow uncertainty on the performance of the optimal rules, which can be taken into account when planning water management for agricultural sustainability and spill control.

Notation

$CropAc_{y,m,cr}$ crop acreage in year y and module m for crop cr: decision variable.

$CP_{y,cr}$ crop price in year y for crop cr: parameter

$Y_{y,m,cr}$ actual yield of crop cr in year y and module m, calculated by the crop production model as a function of irrigation water amount and salinity.

$CS_{y,cr}$ subsidy for crop cr in year y: parameter.

$CC_{y,cr}$ production cost for cr in year y: parameter.

$DC_{y,m}$ water cost for module m in year y, which includes both fixed administrative costs and variable pumping costs; pumping costs depend on actual head drawdowns calculated by the regional groundwater model, plus a correction for in-well drawdown.

α scaling factor: parameter

$Spill_{y,t,k}$ spill in year y, month t, from reservoir k: decision variable.

$CropAcTot$ total irrigable land: parameter.

$Pump_{y,t,w}$ groundwater pumping rate in year y, month t, from well w: decision variable.

$PumpCap_w$ monthly pumping capacity for well w: parameter.

$RO_{y,t,k}$ Yaqui river runoff (streamflow) in year y, month t, into reservoir k: parameter.

$P_{y,t,k}$ rainfall in year y, month t, into reservoir k: parameter.

$E_{y,t,k}$ evaporation in year y, month t, from reservoir k: parameter.

$A_{y,t,k}$ reservoir surface area: calculated as a function of reservoir storage by the reservoir model.

f_c coefficient describing water losses between two sequential reservoirs: parameter.

$Q_{y,t,k}$ release in year y, month t, from reservoir k: decision variable.

$Q^{fix}_{y,t,k}$ fixed reservoir releases for urban users and priority right farmers in the Yaqui Valley, in year y, month t, from reservoir k: parameter.

$S_{\min,k}$ and $S_{\max,k}$ lower and upper limits on monthly storage in reservoir k: parameter.

$CW_{y,t,m}$ surface water demand in year y, month m, from module m.

$Q_{leak,y,t,r}$ irrigation canal seepage loss in year y, month t, from reach r, calculated by the canal model.

$Q_{\min}$ and $Q_{\max}$ lower and upper limits on monthly releases from the downstream reservoir: parameter.

$QA_{\min}$ and $QA_{\max}$ lower and upper limits on annual releases from the downstream reservoir: parameter.

$IrrigEff_{cr}$ irrigation efficiency for crop cr: parameter accounting for nonuniform infiltration at the field scale.

$DP_{y,m,cr}$ deep percolation losses in year y, module m, for crop cr, calculated by the crop production model. accounts for deep percolation losses due to suboptimal crop ET caused by salinity stress.

$AW_{y,m,cr}$ applied water in year y, module m, for crop cr.

$LCH_{\max}$ upper limit on the field-scale leaching fraction for irrigation: parameter.

[48] **Acknowledgments.** We gratefully acknowledge data contributions from the Yaqui Irrigation District and from the CNA in Mexico. We also appreciate valuable insights and data contributions from I. Ortiz-Monasterio. We thank Michael Saunders for providing us with the SNOPT optimization code and giving valuable advice on its use. We thank Jasper Vrugt for providing us with the MOSCEM-UA algorithm. We are most grateful to the David and Lucile Packard Foundation and the UPS Foundation for their generous support of this research. Constructive comments from the Associate Editor and three anonymous reviewers significantly improved the original manuscript.

References

Addams, C. L. (2004), Water resource policy evaluation using a combined hydrological-economic-agronomic modeling framework: Yaqui Valley, Sonora, Mexico, Ph.D. dissertation, 354 pp., Stanford Univ., Stanford, Calif.

Beman, J. M., K. R. Arrigo, and P. A. Matson (2005), Agricultural runoff fuels large phytoplankton blooms in vulnerable areas of the ocean, *Nature*, *434*(7030), 211–214.

Bhaskar, N. R., and E. E. Whitlatch (1980), Derivation of monthly reservoir release policies, *Water Resour. Res.*, *16*, 987–993.

Bredehoeft, J. D., and R. A. Young (1983), Conjunctive use of groundwater and surface water: Risk aversion, *Water Resour. Res.*, *19*, 1111–1121.

Cai, X. M., D. C. McKinney, and L. S. Lasdon (2001), Solving nonlinear water management models using a combined genetic algorithm and linear programming approach, *Adv. Water Resour.*, *24*, 667–676.

Cai, X. M., D. C. McKinney, and L. S. Lasdon (2002), A framework for sustainability analysis in water resources management and application to the Syr Darya Basin, *Water Resour. Res.*, *38*(6), 1085, doi:10.1029/2001WR000214.

Faber, B. A., and J. R. Stedinger (2001), Reservoir optimization using sampling SDP with ensemble streamflow prediction forecasts, *J. Hydrol.*, *249*, 113–133.

Gill, P. E., W. Murray, and M. A. Saunders (2002), SNOPT: An SQP algorithm for large-scale constrained optimization, *SIAM J. Optim.*, *12*(4), 979–1006.

Hiew, K., J. Labadie, and J. Scott (1989), Optimal operational analysis of the Colorado–Big Thompson project, in *Computerized Decision Support Systems for Water Managers*, edited by J. Labadie et al., pp. 632–646, Am. Soc. of Civ. Eng., Reston, Va.

Jacobs, J., G. Freeman, J. Grygier, D. Morton, G. Schultz, K. Staschus, and J. Stedinger (1995), SOCRATES: A system for scheduling hydroelectric generation under uncertainty, *Ann. Oper. Res.*, *59*, 99–134.

Koutsoyiannis, D. (2001), Coupling stochastic models of different time scales, *Water Resour. Res.*, *37*, 379–391.

Labadie, J. W. (2004), Optimal operation of multireservoir systems: State-of-the-art review, *J. Water Resour. Plann. Manage.*, *130*(2), 93–111.

Loaiciga, H. A. (2005), On the probability of droughts: The compound renewal model, *Water Resour. Res.*, *41*, W01009, doi:10.1029/2004WR003075.

Loaiciga, H. A., and M. A. Marino (1986), Risk analysis for reservoir operation, *Water Resour. Res.*, *22*, 483–488.

Loucks, D. P. (2000), Sustainable water resources management, *Water Int.*, *25*(1), 3–10.

Loucks, D. P., and P. Dorfman (1975), An evaluation of some linear decision rules in chance-constrained models for reservoir planning and operation, *Water Resour. Res.*, *11*, 777–782.

Lund, J. R., and I. Ferreira (1996), Operating rule optimization for Missouri River reservoir system, *J. Water Resour. Plann. Manage.*, *122*(4), 287–295.

Maas, E. V. (1990), Crop salt tolerance, in *Agricultural Salinity Assessment and Management*, *Manuals Rep. Eng. Pract.*, vol. 71, edited by K. Tanji, Am. Soc. of Civ. Eng., Reston, Va.

McPhee, J., and W.-G. Yeh (2005), Multiobjective optimization for sustainable groundwater management in semiarid regions, *J. Water Resour. Plann. Manage.*, *130*(6), 490–497.

Naylor, R. L., W. P. Falcon, and A. Puente-Gonzalez (2001), Policy reforms and Mexican agriculture: Views from the Yaqui Valley, *Econ. Program Pap. 01–01*, Cent. Int. de Mejoramiento de Maiz y Trigo, Houston, Tex.

Oliveira, R., and D. P. Loucks (1997), Operating rules for multireservoir systems, *Water Resour. Res.*, *33*, 839–852.

Raman, H., and V. Chandramouli (1996), Deriving a general operating policy for reservoirs using neural network, *J. Water Resour. Plann. Manage.*, *122*(5), 342–347.

Rasmussen, P. F., J. D. Salas, L. Fagherazzi, J. C. Rassam, and B. Bobee (1996), Estimation and validation of contemporaneous PARMA models for streamflow simulation, *Water Resour. Res.*, *32*, 3151–3160.

Reichard, E. G. (1995), Groundwater-surface water management with stochastic surface water supplies: A simulation-optimization approach, *Water Resour. Res.*, *31*, 2845–2865.

Reichard, E. G., and T. A. Johnson (2005), Assessment of regional management strategies for controlling seawater intrusion, *J. Water Resour. Plann. Manage.*, *131*(4), 280–291.

Salas, J. D. (1993), Analysis and modeling of hydrologic time series, in *Handbook of Hydrology*, edited by D. R. Maidment, pp. 19.1–19.72, McGraw-Hill, New York.

Schoups, G., C. L. Addams, and S. M. Gorelick (2005), Multi-objective calibration of a surface water-groundwater flow model in an irrigated agricultural region: Yaqui Valley, Sonora, Mexico, *Hydrol. Earth Syst. Sci.*, *9*, 549–568.

Schoups, G., C. L. Addams, J. L. Minjares, and S. M. Gorelick (2006), Sustainable conjunctive water management in irrigated agriculture: Model formulation and application to the Yaqui Valley, Mexico, *Water Resour. Res.*, *42*, W10417, doi:10.1029/2006WR004922.

Seifi, A., and K. Hipel (2001), Interior-point method for reservoir operation with stochastic inflows, *J. Water Resour. Plann. Manage.*, *127*(1), 48–57.

Srinivas, V. V., and K. Srinivasan (2005), Hybrid moving block bootstrap for stochastic simulation of multi-site multi-season streamflows, *J. Hydrol.*, *302*, 307–330.

Tarboton, D. G., A. Sharma, and U. Lall (1998), Disaggregation procedures for stochastic hydrology based on nonparametric density estimation, *Water Resour. Res.*, *34*(1), 107–119.

Tejada-Guibert, J., S. Johnson, and J. Stedinger (1995), The value of hydrologic information in stochastic dynamic programming models of a multireservoir system, *Water Resour. Res.*, *31*, 2571–2579.

Tsur, Y. (1990), Stabilization role of groundwater when surface water supplies are uncertain: The implications for groundwater development, *Water Resour. Res.*, *26*, 811–818.

Vogel, R. M., and A. L. Shallcross (1996), The moving blocks bootstrap versus parametric time series models, *Water Resour. Res.*, *32*, 1875–1882.

Vrugt, J. A., H. V. Gupta, L. A. Bastidas, W. Bouten, and S. Sorooshian (2003), Effective and efficient algorithm for multiobjective optimization of hydrologic models, *Water Resour. Res.*, *39*(8), 1214, doi:10.1029/2002WR001746.

Willis, R., and B. A. Finney (1988), Planning model for optimal control of saltwater intrusion, *J. Water Resour. Plann. Manage.*, *114*(2), 163–178.

Yeh, W. W. G. (1985), Reservoir management and operations models: A state-of-the-art review, *Water Resour. Res.*, *21*, 1797–1818.

Young, G. K. (1967), Finding reservoir operation rules, *J. Hydraul. Div. Am. Soc. Civ. Eng.*, *93*, 297–321.

Zitzler, E., and L. Thiele (1999), Multi-objective evolutionary algorithms: A comparative case study and the strength Pareto approach, *IEEE Trans. Evol. Comput.*, *3*(4), 257–271.

C. L. Addams, S. M. Gorelick, and G. Schoups, Department of Geological and Environmental Sciences, Stanford University, Stanford, CA 94305, USA. (gerrit.schoups@gmail.com)

J. L. Minjares, Comisión Nacional del Agua, Cuidad Obregón, Sonora CP 85000, Mexico.